doi:10.1016/j.jmb.2010.03.029 J. Mol. Biol. (2010) 398, 614–622

JMB

Available online at www.sciencedirect.com

ScienceDirect

ELSEVIER

Structural and Biochemical Characterization of Yeast Monothiol Glutaredoxin Grx6

Ming Luo[1], Yong-Liang Jiang[1], Xiao-Xiao Ma[1], Ya-Jun Tang[1], Yong-Xing He[1], Jiang Yu[1], Rong-Guang Zhang[2], Yuxing Chen[1] and Cong-Zhao Zhou[1]*

[1]*Hefei National Laboratory for Physical Sciences at Microscale and School of Life Sciences, University of Science and Technology of China, Hefei, Anhui 230027, People's Republic of China*

[2]*Structural Biology Center, Argonne National Laboratory, 9700 South Cass Avenue, Argonne, IL 60439, USA*

Received 6 January 2010; received in revised form 14 March 2010; accepted 17 March 2010
Available online 27 March 2010

Edited by R. Huber

Glutaredoxins (Grxs) are a ubiquitous family of proteins that reduce disulfide bonds in substrate proteins using electrons from reduced glutathione (GSH). The yeast *Saccharomyces cerevisiae* Grx6 is a monothiol Grx that is localized in the endoplasmic reticulum and Golgi compartments. Grx6 consists of three segments, a putative signal peptide (M1-I36), an N-terminal domain (K37-T110), and a C-terminal Grx domain (K111-N231, designated Grx6C). Compared to the classic dithiol glutaredoxin Grx1, Grx6 has a lower glutathione disulfide reductase activity but a higher glutathione *S*-transferase activity. In addition, similar to human Grx2, Grx6 binds GSH via an iron–sulfur cluster *in vitro*. The N-terminal domain is essential for noncovalent dimerization, but not required for either of the above activities. The crystal structure of Grx6C at 1.5 Å resolution revealed a novel two-strand antiparallel β-sheet opposite the GSH binding groove. This extra β-sheet might also exist in yeast Grx7 and in a group of putative Grxs in lower organisms, suggesting that Grx6 might represent the first member of a novel Grx subfamily.

Keywords: glutaredoxin; *Saccharomyces cerevisiae*; crystal structure; enzymatic activity; glutathione *S*-transferase

Introduction

Loss of redox homeostasis leads to accumulation of reactive oxygen species that can be harmful to cells. In addition to the thioredoxins (Trxs), a group of glutathione (GSH)-dependent oxidoreductases called glutaredoxins (Grxs) also function in maintaining this homeostasis.[1,2] Primary sequence alignment easily distinguishes most Grxs from Trxs. However, from the viewpoint of three-dimensional (3-D) structure, Grxs share a highly similar fold and topology with the Trx family†,[3] which is characterized by a central β-pleated sheet surrounded by five helices and a CXX(C/S) active-site motif.[1,4] As previously reported, Grxs carry out a number of biological functions, including reduction of ascorbate, activation of ribonucleotide reductase and 3′-phosphoadenylylsulfate reductase, and regulation of the DNA-binding capacity of nuclear factors.[4,5] Recently, however, a variety of Grxs or Grx-like proteins were found that execute distinct functions, such as signal transduction and iron–sulfur (Fe–S) cluster assembly.[5,6]

The genome of the yeast *Saccharomyces cerevisiae* encodes multiple Grx isoforms, making it an ideal model for exploring the diversity of Grx subcellular localizations and molecular functions. To date, eight Grxs have been found in yeast, named Grx1 to Grx8 in chronological order of identification‡. Grx1/YCL035C and Grx2/YDR513W are dithiol cytosolic Grxs that contain a conserved CPYC motif at the active site. Deletion of *GRX1* or *GRX2* will lead to some sort of sensitivity to superoxide anions and

**Corresponding author.* E-mail address: zcz@ustc.edu.cn.

† http://pfam.sanger.ac.uk

Abbreviations used: β-ME-SG, glutathionylated β-mercaptoehanol; Fe–S, iron–sulfur; GR, glutathione reductase; Grx, glutaredoxin; Grx6C, C-terminal domain of Grx6; GSH, reduced glutathione; GSSG, glutathione disulfide; GST, glutathione *S*-transferase; HEDS, bis-(2-hydroxyethyl)-disulfide; NBD-Cl, 4-chloro-7-nitro-2,1,3-benzoxadiazole; PDB, Protein Data Bank; Trx, thioredoxin.

‡ http://www.yeastgenome.org/

hydrogen peroxide, respectively, suggesting their different roles in protecting the yeast cells from oxidative stress.[7] Grx1 exists mostly in the cytoplasm. Upon reduction, its residues around the active site undergo conformational changes that reinforce GSH binding.[8] Grx2 is expressed in two isoforms via alternative translation using different start codons, with the full-length version translocated to the mitochondrial matrix and the truncated version retained in the cytosol.[9,10] In contrast to these two typical dithiol Grxs, the monothiol Grxs, Grx3/YDR098C, Grx4/YER174C, and Grx5/YPL059W, have an active site with the CGFS motif.[11] Grx3 and Grx4 are required for the regulation of the iron-dependent transcriptional factor Aft1 in the nucleus,[12] and Grx5 is involved in the synthesis or assembly of Fe–S clusters in the mitochondrial matrix.[13,14]

In addition to these five well-known yeast Grxs, three new members, Grx6/YDL010W, Grx7/YBR014C, and Grx8/YLR364W were recently identified.[15] Grx6 and Grx7 are monothiol Grxs, with an active-site motif of CSYS in Grx6 and of CPYS in Grx7. These Grxs were proposed to be responsible for regulating the sulfhydryl redox state in the oxidative conditions of early secretory pathway vesicles.[16] Heterogeneously expressed Grx6 and Grx7 have glutathione disulfide (GSSG) reductase activity, as detected by the GSH–HEDS [bis-(2-hydroxyethyl)-disulfide transhydrogenase] assay.[17] However, Grx6 is localized in both the endoplasmic reticulum and Golgi apparatus, while Grx7 is found mostly in the Golgi apparatus. Grx6, but not Grx7, binds two [2Fe–2S] clusters to form a tetramer *in vitro*.[17] In addition to Grx1 and Grx2, Grx8 is a third putative dithiol Grx, encoded by *GRX8/YLR364W*, which does not affect growth rate under oxidative stress conditions when deleted.[18] The apparent K_{cat} for Grx7 in the HEDS assay is about 1000-fold higher than that for Grx8, even though their apparent K_m values are comparable.[18]

To systematically explore structural insights into the diverse functions of Grxs, we initiated a project to solve the 3-D structures of all eight yeast Grxs. In addition to previous reports for Grx1 [under the Protein Data Bank (PDB) codes of 3C1R and 3C1S],[8] Grx2 (PDB codes 3CTF and 3CTG), and Grx5 (PDB code 3GX8),[19] we present here the biochemical characterization of Grx6, and the crystal structure of its C-terminal Grx domain (designated Grx6C). Full-length Grx6 and Grx6C possess similar GSSG reductase activities (EC 1.8.1.7) and glutathione *S*-transferase (GST) activities (EC 2.5.1.18), and the crystal structure of Grx6C at 1.5 Å resolution revealed a novel two-strand antiparallel β-sheet motif inserted into the classical Grx domain. Further structure-based multiple alignments of Grx6 against its bacterial and fungal homologs enabled us to define a new subfamily of Grxs.

Results

The organization of Grx6

Grx6 is composed of three segments, a putative signal peptide (M1-I36), an N-terminal domain

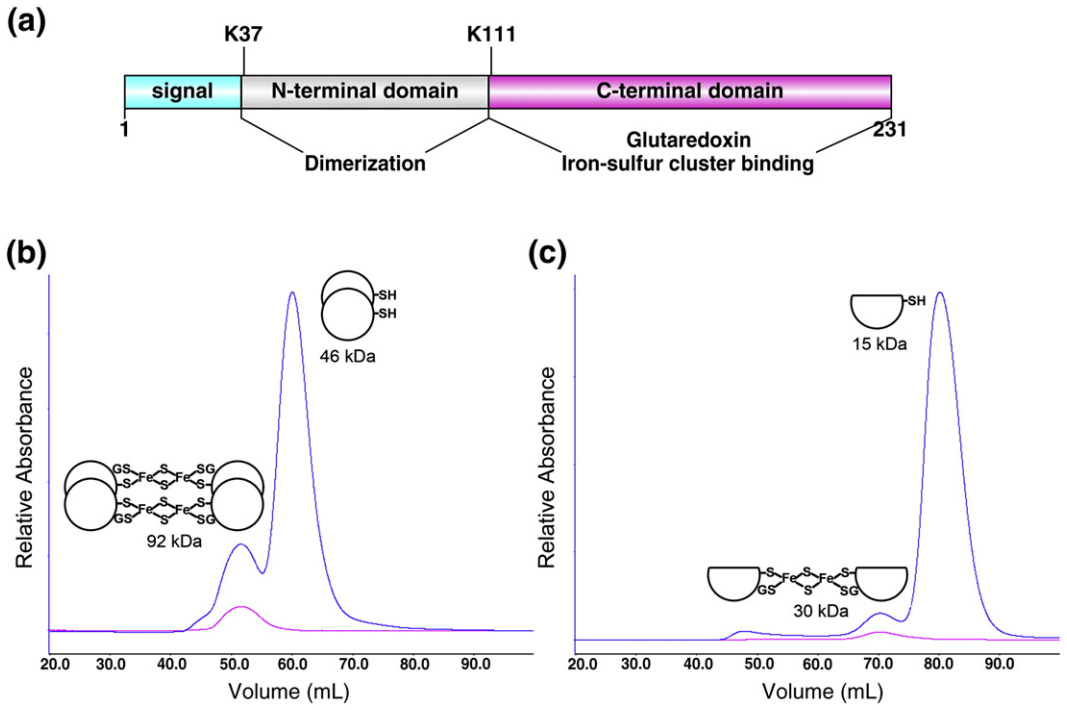

Fig. 1. The organization of Grx6. (a) Three segments of Grx6 drawn by Domain Graph, version 1.0.[20] Signal peptide, N- and C-terminal domains are shown in cyan, gray and pink, respectively. Gel-filtration chromatography of (b) Grx6 and (c) Grx6C. The blue and pink chromograms represent the absorbance at 280 and 430 nm, respectively. A schematic diagram of each oligomer is shown at the corresponding peak.

Table 1. Apparent steady-state kinetic constants of yeast Grxs

	β-ME-SG		
Protein	K_m (mM)	K_{cat} (S^{-1})	K_{cat}/K_m ($\times 10^4$ M^{-1} S^{-1})
Grx1	0.19	14.35	7.55
Grx7	0.40	29.52	7.38
Grx6	2.95	37.31	1.26
Grx6C	3.02	37.82	1.25

The reaction mix contained 100 mM Tris–HCl (pH 7.5), 3 mM GSH, 0.25 mM NADPH, and yeast GR (6 μg/mL). HEDS concentration varied from 0.1 to 2.5 mM; reactions were started by addition of the indicated Grx to a final concentration of 40 nM.

(K37-T110), and a C-terminal Grx domain (K111-N231) (Fig. 1a). The signal peptide might be responsible for its subcellular localization in the endoplasmic reticulum and Golgi apparatus, as predicted by SignalP 3.0 Server§.[21] Gel-filtration chromatography showed that freshly purified Grx6 was eluted at two peaks corresponding to apparent molecular masses of 46 kDa (dimer) and 92 kDa (tetramer) (Fig. 1b). However, only the tetrameric form shows a strong absorbance at 430 nm, which features the [2Fe–2S] cluster.[17] In contrast, Grx6C was eluted at two volumes corresponding to 15 kDa (monomer) and 30 kDa (dimer), with only the dimeric form showing the characteristic absorbance at 430 nm (Fig. 1c). These gel-filtration profiles indicated that the C-terminal Grx domain (K111-N231) is responsible for assembly of the Fe–S cluster, whereas the N-terminal domain (K37-T110) plays a crucial role in dimerization of the Grx6 monomer. In addition, trypsin digestion could completely remove the N-terminal domain (data not shown), suggesting it exists as a more protease-sensitive segment, independent of the C-terminal Grx domain.

GSSG reductase activity

Grxs have traditionally been classified by their ability to reduce the mixed disulfide of glutathionylated β-mercaptoehanol (β-ME-SG).[22] The typical dithiol Grxs, Grx1 and Grx2, are capable of reducing the mixed disulfide.[7] In contrast, the five yeast monothiol Grxs have been divided into two groups, with Grx6-7, but not Grx3-5, having this activity.[17]

In addition to systematic kinetic analyses of Grx7 reported by Mesecke *et al.*,[17] we found that both Grx6 and Grx6C possess HEDS activity, with a maximum reaction velocity (V_{max}) proportional to enzyme concentration at approximately 40 nM. Using yeast Grx1 and Grx7 as positive controls, we obtained kinetic data for Grx6 and Grx6C that could be well fitted to Michaelis–Menten kinetics. As summarized in Table 1, compared to Grx1, Grx6 has higher K_m and K_{cat} values toward β-ME-SG, resulting in a lower catalytic efficiency (K_{cat}/K_m) of approximately one-sixth that of Grx1. Moreover, compared to Grx7, Grx6 has a higher K_m and a similar K_{cat}, leading to a lower K_{cat}/K_m, despite a sequence identity of up to 52% in the Grx domain. Grx6C shows K_m and K_{cat} values similar to that of Grx6, indicating the N-terminal domain contributes little to the HEDS activity.

§ http://cbs.dtu.dk/services/SignalP/

GST activity

GSTs belong to a family of proteins mainly involved in the detoxification of xenobiotic compounds by conjugation to the sulfhydryl group of GSH, which is activated to reactive thiolate form by residues around the active site.[23] In addition to classical GSTs, some Grxs also catalyze this conjugation. For example, both *in vitro* and *in vivo* experiments demonstrated that the dithiol Grxs, Grx1 and Grx2, whose sequence corresponds to the N-terminal domain of classical GSTs, possess GST activity.[24] However, whether the monothiol Grxs, Grx6 and Grx7, have this activity is unknown.

With Grx1, Grx2, and glutathione *S*-transferase Gtt2[25] as controls, the GST activities of Grx6, Grx6C, and Grx7 were detected by monitoring at 419 nm for the conversion of 4-chloro-7-nitro-2,1,3-benzoxadiazole (NBD-Cl) to glutathionylated NBD. As shown in Fig. 2, Grx6 possesses GST activity at a catalytic velocity of approximately three- or four-fold that of Grx1 or Grx2, but only one-seventh that of Gtt2. In contrast, Grx7 has a catalytic velocity similar to that of Grx2. In addition, Grx6C had a

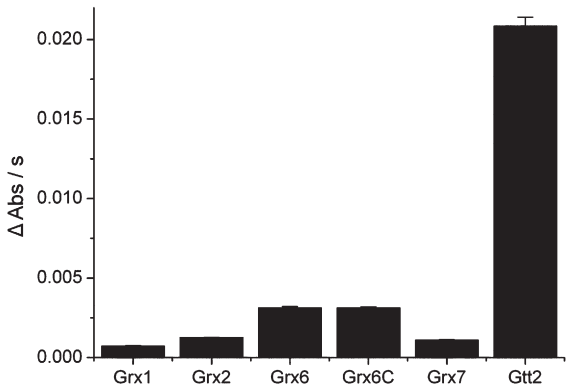

Fig. 2. GST activity assays. Assays for Grx1, Grx2, Grx6, Grx6C, Grx7, and Gtt2 were performed in 0.5 mM NBD-Cl, 2 mM GSH, and the indicated enzyme at a final concentration of 10 μM. Shown are histograms of enzymatic activity.

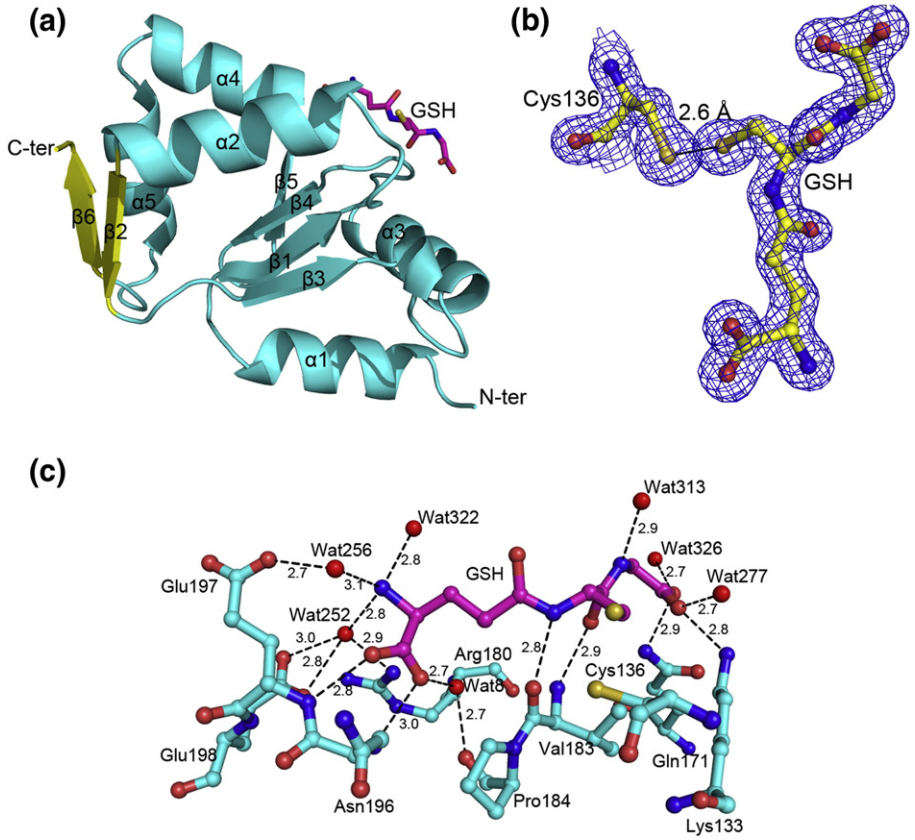

Fig. 3. Overall structure of Grx6C and GSH-binding site. (a) Representation of Grx6C binding to GSH. Secondary structures are labeled. (b) σ_A-weighted $2F_o-F_c$ density map of GSH. (c) Stereo representation of the GSH–Grx6C interactions. Grx6C atoms are C, cyan; S, gold; O, red; and N, blue. GSH atoms are C, pink; S, gold; O, red; and N, blue. Water is red. Hydrogen bonds are indicated by dashed lines, with atomic distances in angstroms.

catalytic velocity almost identical to that of Grx6, indicating the N-terminal domain was not involved in the GST activity.

Overall structure of Grx6C

To better understand the structural basis of these activities, we applied the 46 -kDa dimer of Grx6 (K37-N231) for crystallization and obtained a crystal that diffracted at 1.5 Å resolution. However, after data processing and structure solution, only Grx6C could be built into the final model. The N-terminal domain may have been degraded during crystallization, with Phe113 as the most N-terminal residue that could be traced in the electron density map. SDS electrophoresis in combination with mass spectrometry analysis of the dissolved crystal confirmed degradation of the N-terminal segment prior to Arg108 or Lys111.

The overall architecture of Grx6C resembles the typical Grx fold of a core four-strand antiparallel β-sheet surrounded by five α-helices (Fig. 3a). In contrast to the typical Grxs, a two-strand antiparallel β-sheet (β2 and β6) was seen opposite the GSH-binding groove. Structural superpositions against all Grx structures in PDB‖ revealed that this two-strand antiparallel β-sheet is unique to Grx6.

GSH-binding site

A GSH molecule fit well in the structure of Grx6C, as shown in the σ_A-weighted $2F_o-F_c$ density map (Fig. 3b). The distance between the sulfur atoms of GSH and Cys136 of Grx6C is about 2.6 Å, which is too far to form a typical disulfide bond (2.0 Å). However, both the shape and the charge of the conserved GSH-binding groove are perfectly complementary to the nestled GSH molecule. The carboxyl group of the glutamyl moiety forms two direct hydrogen bonds with the N^{α} atoms of Asn196 and Glu197, and an indirect hydrogen bond with the carboxyl oxygen of Pro184 via the water molecule Wat8 (Fig. 3c). The N^{α} of the glutamyl moiety interacts with Glu197$O^{\varepsilon 1}$ through Wat256 and forms two hydrogen bonds with Glu198$O^{\varepsilon 1}$ and $O^{\varepsilon 2}$ atoms through Wat252. The N^{α} of the cysteinyl moiety forms a hydrogen bond with the Val183 carboxyl oxygen, and the cysteinyl carboxyl oxygen forms a hydrogen bond with the N^{α} of Val183. The carboxyl group of the glycinyl moiety is fixed by polar interactions with the side chains of Lys133 and Gln171, and hydrogen-bonds with two water molecules, Wat277 and Wat326. In addition, the

‖http://www.rcsb.org/pdb

N^{α} of the glycinyl moiety forms a hydrogen bond with Wat313.

Discussion

N-terminal-mediated noncovalent dimerization of Grx6 and Fe–S cluster-mediated covalent dimerization of Grx6C

Several Grxs form noncovalently linked homodimers, such as *Trypanosoma brucei* Grx1,[26] poplar GrxC4,[27] and *Escherichia coli* Grx1.[28] The poplar GrxC4 homodimer has a novel dimerization interface formed largely by hydrophobic interactions that bury the three α-helices around the active site.[27] Grx6 and Grx7 form noncovalently linked homodimers *in vitro*, independent of GSH/GSSG, and Grx6 further forms a dimer of dimers bridged by the Fe–S cluster.[17]

As shown by gel-filtration chromatography, the leading elution peaks represent the tetrameric form for Grx6 (Fig. 1b) and the dimeric form for Grx6C (Fig. 1c), which resulted from Fe–S cluster binding. Grx6C and Grx6 have similar A_{280nm}/A_{430nm} absorbance ratios of (Fig. 1b and c), indicating the dimers of Grx6C were predominantly formed by Fe–S cluster interactions, rather than through direct intermolecular interface. Thus, we propose that the noncovalent dimerization of Grx6 depends on its N-terminal domain (Fig. 1a and b). In addition, the fraction containing the Fe–S cluster was much

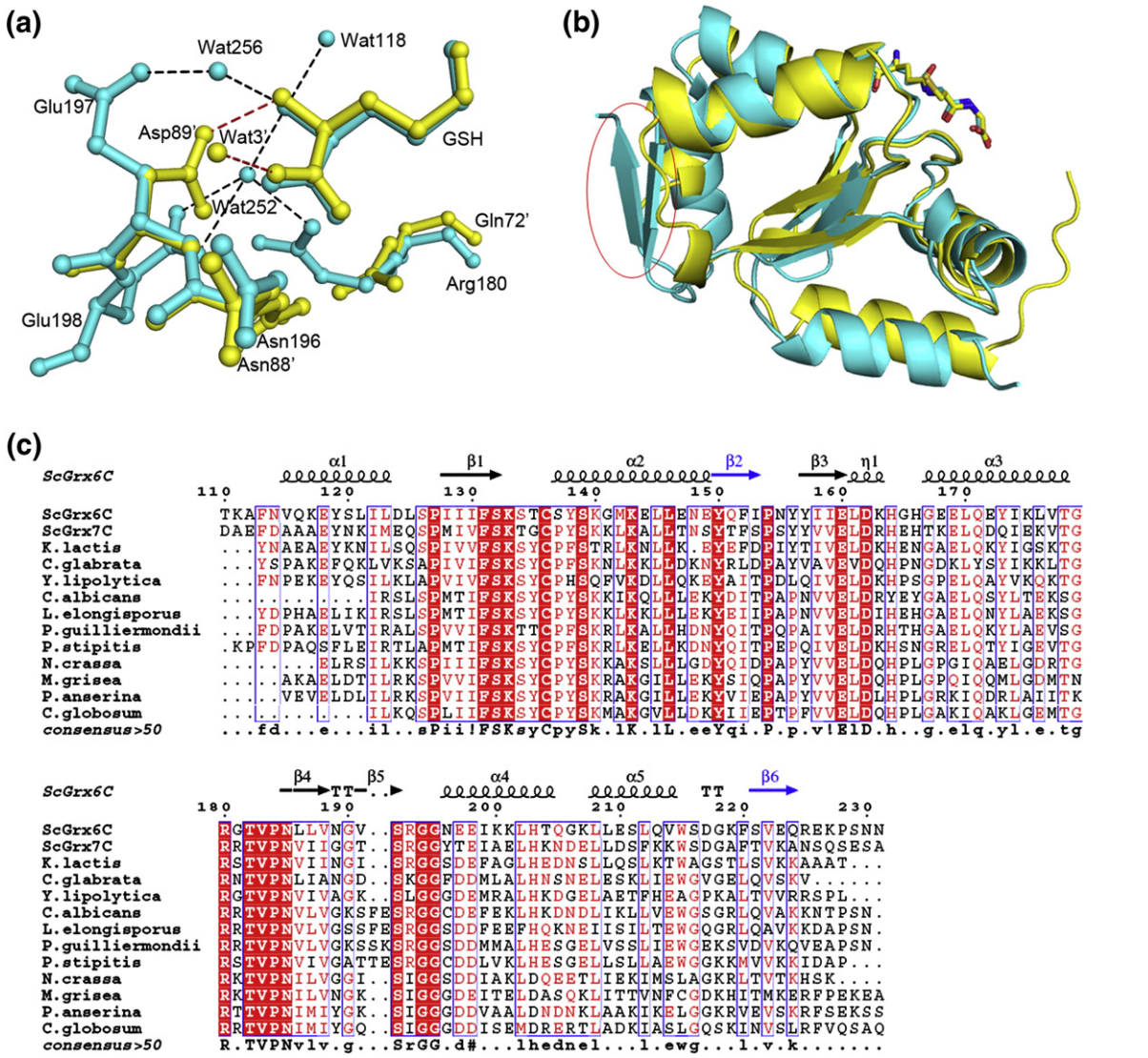

Fig. 4. Comparison of Grx6 and Grx1. (a) Differences in GSH-binding sites between Grx6C (cyan) and Grx1 (yellow). (b) Superposition of Grx6C (cyan) and Grx1 (yellow). (c) Comparison of Grx6C and Grx7C sequences with Grx-fold proteins (GenBank accession numbers in parentheses) from *Kluyveromyces lactis* (CAG99837), *Candida glabrata* (CAG60384), *Yarrowia lipolytica* (CAG78790), *Candida albicans* (EAK92123), *Lodderomyces elongisporus* (EDK45643), *Pichia guilliermondii* (EDK39230), *Pichia stipitis* (ABN65676), *Neurospora crassa* (EAA35931), *Magnaporthe grisea* (EDK05786), *Podosporaanserina* (CAP67785), and *Chaetomium globosum* (EAQ89239) using MultAlin[36] and ESPript[37] (http://prodes.toulouse.inra.fr/multalin). The secondary structural elements of Grx6C are displayed above.

greater in the intact Grx6 sample (Fig. 1b) than that in the Grx6C sample (Fig. 1c), indicating that dimerization mediated by the N-terminal domain may facilitate stabilization of the Fe–S cluster.

Is Grx6 a trifunctional protein?

Fe–S clusters are ubiquitous and evolutionarily ancient prosthetic groups that are required to sustain fundamental life processes.[29] Yeast Grx5 and Grx6, human Grx2 and Grx5, poplar GrxC1, *T. brucei* Grx1, and *E. coli* Grx4 all bind the Fe–S cluster, most likely a [2Fe–2S] cluster.[17,26,30–33] The crystal structures of human Grx2 (PDB code 2HT9) and poplar GrxC1 (PDB code 2E7P) in the holo form show that incorporation of the Fe–S cluster requires not only the Grx dimer, but also two GSH molecules.[32,34] Human Grx2 is primarily present in the holo form, which is inactive under normal conditions, but is activated *in vitro* by GSSG following the loss of the cofactor [2Fe–2S] cluster, or *in vivo* by a decrease in the GSH/GSSG ratio.[30] The activated human Grx2 uses GSH as an electron donor to reduce low-molecular-mass disulfide molecules and protein GSH-mixed disulfides.[35] *E. coli* Grx4 undergoes dramatic conformational changes to release the intact [2Fe–2S] cluster, which is thought to be transferred to acceptor proteins.[33]

Similar to human Grx2 and *E. coli* Grx4, when Grx6 is in the Fe–S cluster form, the single cysteine Cys136 coordinates with the iron, and the protein is inactive. However, whether Grx6 serves as a redox sensor or as an Fe–S cluster storage protein remains unknown. When the GSH/GSSG ratio decreases, the HEDS or GST activity of Grx6 could be restored by the loss of the Fe–S cluster. This would lead to recognition of the GSH molecule by the GSH-binding groove and transfer of the electron to Cys136. Therefore, in addition to its HEDS and GST activities, Grx6 may be the first trifunctional protein of the yeast Grx family.

Grx6 may be the first member of a novel Grx subfamily

To the best of our knowledge, Grx6 and Grx7 are the only two monothiol Grxs with GSSG reductase activity in the HEDS assay. These results are in agreement with the 3-D structure of Grx6C, which is clearly distinct from that of other yeast monothiol Grxs and more closely related to that of dithiol Grx1 and Grx2. Compared to Grx1, Grx6 has a lower catalytic efficiency toward HEDS but a higher GST activity. These differences might be due to variations at the GSH-binding site (Fig. 4a).

Superposition of Grx6 on Grx1 shows homologous secondary structures, except for the extra two-strand antiparallel β-sheet (Fig. 4b). This β-sheet has never been reported before in Grxs of known structure. Sequence alignment showed that this β-sheet is not conserved in other yeast Grxs, except for Grx7. However, a sequence homology search of Grx6C against the nonredundant protein sequence database¶ yielded a group of proteins with a similar Grx-fold. Multialignment of these protein sequences indicated that the tyrosine and proline residues flanking the β2-strand are highly conserved, and a longer C-terminus is crucial for forming the β6-strand, which is indispensable for forming the extra β-sheet (Fig. 4c). To further validate the essential nature of β6, we constructed three truncated versions of Grx6C by deleting the C-terminal 13 (β6 completely deleted), 10 (β6 partially deleted), or 7 residues (β6 retained). Both the 13- and 10-residue deleted versions were expressed as inclusion bodies, while the 7-residue deletion was soluble (data not shown). These results indicated that the β6-strand is critical for the proper folding of Grx6C during overexpression in *E. coli*. Together, these results show that the putative members of Grx that have an extra β-sheet might represent a novel Grx subfamily.

Conclusion

We showed that Grx6 can bind an Fe–S cluster through its C-terminal Grx domain and form noncovalently linked dimers through its N-terminal domain. Compared with the classic dithiol glutaredoxin Grx1, Grx6 has a lower HEDS activity but a higher GST activity. Similar to human Grx2, Grx6 also binds GSH via an Fe–S cluster *in vitro*. The structure of the C-terminal glutaredoxin domain of Grx6 revealed an extra two-strand antiparallel β-sheet, opposite the GSH-binding groove, a unique motif among Grxs. Grx6 appears to be the first identified member of a novel Grx subfamily.

Materials and Methods

Cloning, expression, and purification of Grx6

The coding regions of Grx6/YDL010W without the signal peptide (residues K37-N231, designated as Grx6) and the C-terminal Grx domain (residues K111-N231, Grx6C) (Fig. 1a) were PCR-amplified from *S. cerevisiae* S288c genomic DNA and cloned into the pET22b vector (Novagen). Extra sequences encoding residues LEHHHHHH were added at the C-terminal. These plasmids were transformed into *E. coli* strain Rosetta (DE3) and induced with 0.02 mM IPTG at 16 °C for 20 h after the OD_{600nm} reached 0.6. Cells were collected by centrifugation and resuspended in buffer A (200 mM NaCl, 20 mM Tris–HCl, pH 8.0). After 3 min of sonication followed by centrifugation at 20,000*g* for 30 min, the supernatant was pooled and loaded onto a Ni-NTA column (GE Healthcare). The target protein was eluted with 250 mM imidazole and loaded onto a Superdex 75 16/60 column preequilibrated with buffer A. Fractions containing recombinant Grx6 were pooled, desalted, and concentrated to 10 mg/mL in a final solution of 50 mM NaCl and 20 mM Tris–HCl (pH 8.0) for crystal screening. Protein concentration was calculated by UV absorbance at 280 nm with an extinction coefficient of 0.695 M^{-1} cm^{-1}[a].

¶ www.ncbi.nlm.nih.gov/BLAST

[a] http://www.expasy.org/tools/protparam.html

Crystallization, data collection, structure solution, and refinement of Grx6

Crystals of selenium-methionine-labeled protein were grown at 16 °C in a hanging drop of 1.0-μl protein sample, prepared as described above, with an equal volume of reservoir solution. After about 1 week, prismatic crystals appeared in the 19% polyethylene glycol monomethyl ether 5000, 0.1 M 2-(*N*-morpholino)-ethane sulfonic acid (pH 6.5), and 10 mM GSH conditions. A single crystal was transferred to cryoprotectant reservoir solution supplemented with 25% glycerol and flash-cooled with liquid nitrogen. X-ray diffraction data were collected at 100 K in a liquid nitrogen stream using synchrotron radiation (Argonne, IL). The data sets were processed and scaled using HKL2000.[38] The phase was determined by single-wavelength anomalous dispersion.[39] The initial model was further refined by manual and automatic rebuilding using Autobuild from the PHENIX program package.[40] The final model was obtained after several rounds of manual rebuilding and refinement using Coot[41] and Refmac5[42] from the CCP4i package, and checked using the program MolProbity[43] and PROCHECK.[44] Data collection and refinement statistics are in Table 2.

HEDS assays

Glutathione-disulfide reductase activity was measured by reduction of mixed disulfides between HEDS and GSH.[22] Steady-state kinetics of yeast enzymes (Grx1, Grx6, Grx6C, and Grx7) were monitored at 30 °C with a DU800 UV–visible spectrophotometer (Beckman Coulter). Stock solutions of 50 mM NADPH, 100 mM GSH, yeast glutathione reductase (GR; 0.6 mg/mL) (Sigma-Aldrich), and 70 mM HEDS were freshly prepared in 0.1 M Tris–HCl (pH 7.5). The reaction mix contained 0.25 mM NADPH, 1 mM GSH, GR (6 μg/mL), 0.7 mM HEDS, and 40 nM Grx. NADPH, GSH, and HEDS were preincubated for 2 min before GR was added, and the assay started by the addition of Grx. Decrease in absorbance at 340 nm was monitored to indicate NADPH consumption.

Activity and substrate specificity toward glutathionylated substrates were determined using 0.1-2.5 mM HEDS in a mixture of 100 mM Tris–HCl (pH 7.5), 3 mM GSH, 0.25 mM NADPH, and GR (6 μg/mL). The reaction was triggered by adding Grx to 40 nM. Independent experiments were performed under three different substrate concentrations; the apparent K_m was calculated by nonlinear regression of Michaelis–Menten plots and K_{cat} by linear regression of the Lineweaver–Burk plots.

Table 2. Crystal parameters, data collection, and structure refinement

	Parameters
Data collection	
Wavelength (Å)	0.9792
Space group	$P2_12_12_1$
Unit cell (Å, °)	$a=50.56$, $b=57.13$, $c=59.10$ $\alpha=\beta=\gamma=90.00$
Resolution range (Å)	50.00–1.50 (1.53–1.50)[a]
Unique reflections	27,154 (1301)
Completeness (%)	96.7 (94.1)
$\langle I/\sigma(I)\rangle$	35.13 (2.26)
R_{merge} (%)[b]	7.7 (67.1)
Average redundancy	9.3 (7.3)
Structure refinement	
Resolution range (Å)	25.72–1.50
R-factor[c]/R_{free}[d] (%)	17.94/20.04
No. of protein atoms	913
No. of water atoms	149
RMSD bond lengths (Å)[e]	0.01
RMSD bond angles (°)	1.23
Mean *B*-factors (Å^2)	18.57
Ramachandran plot (residues, %)[f]	
Most favored (%)	100
Additional allowed (%)	0
Outliers (%)	0
PDB entry	3L4N

[a] The values in parentheses refer to statistics in the highest bin.
[b] $R_{merge}=\sum_{hkl}\sum_i|I_i(hkl)-\langle I(hkl)\rangle|/\sum_{hkl}\sum_i I_i(hkl)$, where $I_i(hkl)$ is the intensity of an observation and $\langle I(hkl)\rangle$ is the mean value for its unique reflection. Summations are over all reflections.
[c] *R*-factor $=\sum_h|F_o(h)-F_c(h)|/\sum_h F_o(h)$, where F_o and F_c are the observed and calculated structure-factor amplitudes, respectively.
[d] R_{free} was calculated with 5% of the data excluded from the refinement.
[e] RMSD from ideal values.
[f] Categories were defined by Molprobity.

GST assays

GST activity was assayed according to the method of Ricci *et al.*,[45] which follows the conjugation of NBD-Cl with GSH as catalyzed by GST and produces a stable yellow compound with a strong absorbance at 419 nm. GST activities of Grx6, Grx6C, and Grx7 were determined with yeast Grx1, Grx2, and GST Gtt2 as positive controls. Stock solutions of 100 mM NBD-Cl and 100 mM GSH were freshly prepared. The assay mix contained 0.5 mM NBD-Cl and 2 mM GSH. The final concentration of enzyme was 2–10 μM. The assay was started by the addition of NBD-Cl and monitored at 419 nm with a DU800 UV–visible spectrophotometer at 25 °C.

PDB accession numbers

Coordinates and structure factors of *S. cerevisiae* Grx6 C-terminal domain have been deposited in the PDB under the accession number 3L4N.

Acknowledgements

This work was supported by the Ministry of Science and Technology of China (Projects 2006CB910202 and 2006CB806501) and the National Natural Science Foundation of China (Program 30870490). We are grateful to all the developers of CCP4 Suit, PHENIX, and ESPript, Dr. L. D. Warren for providing PyMOL, and Dr. Xue Yu for the program Domain Graph.

References

1. Holmgren, A. (1989). Thioredoxin and glutaredoxin systems. *J. Biol. Chem.* **264**, 13963–13966.
2. Holmgren, A., Johansson, C., Berndt, C., Lonn, M. E., Hudemann, C. & Lillig, C. H. (2005). Thiol redox control via thioredoxin and glutaredoxin systems. *Biochem. Soc. Trans.* **33**, 1375–1377.

3. Finn, R. D., Mistry, J., Tate, J., Coggill, P., Heger, A., Pollington, J. E. *et al.* (2010). The Pfam protein families database. *Nucleic Acids Res.* **38**, D211–222.
4. Fernandes, A. P. & Holmgren, A. (2004). Glutaredoxins: glutathione-dependent redox enzymes with functions far beyond a simple thioredoxin backup system. *Antioxid. Redox Signal.* **6**, 63–74.
5. Herrero, E. & de la Torre-Ruiz, M. A. (2007). Monothiol glutaredoxins: a common domain for multiple functions. *Cell. Mol. Life Sci.* **64**, 1518–1530.
6. Herrero, E., Ros, J., Tamarit, J. & Belli, G. (2006). Glutaredoxins in fungi. *Photosynth. Res.* **89**, 127–140.
7. Luikenhuis, S., Perrone, G., Dawes, I. W. & Grant, C. M. (1998). The yeast *Saccharomyces cerevisiae* contains two glutaredoxin genes that are required for protection against reactive oxygen species. *Mol. Biol. Cell*, **9**, 1081–1091.
8. Yu, J., Zhang, N. N., Yin, P. D., Cui, P. X. & Zhou, C. Z. (2008). Glutathionylation-triggered conformational changes of glutaredoxin Grx1 from the yeast *Saccharomyces cerevisiae*. *Proteins*, **72**, 1077–1083.
9. Porras, P., Padilla, C. A., Krayl, M., Voos, W. & Barcena, J. A. (2006). One single in-frame AUG codon is responsible for a diversity of subcellular localizations of glutaredoxin 2 in *Saccharomyces cerevisiae*. *J. Biol. Chem.* **281**, 16551–16562.
10. Pedrajas, J. R., Porras, P., Martinez-Galisteo, E., Padilla, C. A., Miranda-Vizuete, A. & Barcena, J. A. (2002). Two isoforms of *Saccharomyces cerevisiae* glutaredoxin 2 are expressed in vivo and localize to different subcellular compartments. *Biochem. J.* **364**, 617–623.
11. Rodriguez-Manzaneque, M. T., Ros, J., Cabiscol, E., Sorribas, A. & Herrero, E. (1999). Grx5 glutaredoxin plays a central role in protection against protein oxidative damage in *Saccharomyces cerevisiae*. *Mol. Cell Biol.* **19**, 8180–8190.
12. Ojeda, L., Keller, G., Muhlenhoff, U., Rutherford, J. C., Lill, R. & Winge, D. R. (2006). Role of glutaredoxin-3 and glutaredoxin-4 in the iron regulation of the Aft1 transcriptional activator in *Saccharomyces cerevisiae*. *J. Biol. Chem.* **281**, 17661–17669.
13. Rodriguez-Manzaneque, M. T., Tamarit, J., Belli, G., Ros, J. & Herrero, E. (2002). Grx5 is a mitochondrial glutaredoxin required for the activity of iron/sulfur enzymes. *Mol. Biol. Cell*, **13**, 1109–1121.
14. Lill, R. & Muhlenhoff, U. (2006). Iron-sulfur protein biogenesis in eukaryotes: components and mechanisms. *Annu. Rev. Cell Dev. Biol.* **22**, 457–486.
15. Mesecke, N., Spang, A., Deponte, M. & Herrmann, J. M. (2008). A novel group of glutaredoxins in the *cis*-Golgi critical for oxidative stress resistance. *Mol. Biol. Cell*, **19**, 2673–2680.
16. Izquierdo, A., Casas, C., Muhlenhoff, U., Lillig, C. H. & Herrero, E. (2008). *Saccharomyces cerevisiae* Grx6 and Grx7 are monothiol glutaredoxins associated with the early secretory pathway. *Eukaryot. Cell*, **7**, 1415–1426.
17. Mesecke, N., Mittler, S., Eckers, E., Herrmann, J. M. & Deponte, M. (2008). Two novel monothiol glutaredoxins from *Saccharomyces cerevisiae* provide further insight into iron–sulfur cluster binding, oligomerization, and enzymatic activity of glutaredoxins. *Biochemistry*, **47**, 1452–1463.
18. Eckers, E., Bien, M., Stroobant, V., Herrmann, J. M. & Deponte, M. (2009). Biochemical characterization of dithiol glutaredoxin 8 from *Saccharomyces cerevisiae*: the catalytic redox mechanism redux. *Biochemistry*, **48**, 1410–1423.
19. Wang, Y., He, Y. X., Yu, J. & Zhou, C. Z. (2009). Cloning, overproduction, purification, crystallization and preliminary X-ray diffraction analysis of yeast glutaredoxin Grx5. *Acta Crystallogr., Sect. F: Struct. Biol. Cryst. Commun.* **65**, 651–653.
20. Ren, J., Wen, L., Gao, X., Jin, C., Xue, Y. & Yao, X. (2009). DOG 1.0: illustrator of protein domain structures. *Cell Res.* **19**, 271–273.
21. Emanuelsson, O., Brunak, S., von Heijne, G. & Nielsen, H. (2007). Locating proteins in the cell using TargetP, SignalP and related tools. *Nat. Protoc.* **2**, 953–971.
22. Holmgren, A. & Aslund, F. (1995). Glutaredoxin. *Methods Enzymol.* **252**, 283–292.
23. Sheehan, D., Meade, G., Foley, V. M. & Dowd, C. A. (2001). Structure, function and evolution of glutathione transferases: implications for classification of non-mammalian members of an ancient enzyme superfamily. *Biochem. J.* **360**, 1–16.
24. Collinson, E. J. & Grant, C. M. (2003). Role of yeast glutaredoxins as glutathione *S*-transferases. *J. Biol. Chem.* **278**, 22492–22497.
25. Ma, X. X., Jiang, Y. L., He, Y. X., Bao, R., Chen, Y. & Zhou, C. Z. (2009). Structures of yeast glutathione-*S*-transferase Gtt2 reveal a new catalytic type of GST family. *EMBO Rep.* **10**, 1320–1326.
26. Comini, M. A., Rettig, J., Dirdjaja, N., Hanschmann, E. M., Berndt, C. & Krauth-Siegel, R. L. (2008). Monothiol glutaredoxin-1 is an essential iron-sulfur protein in the mitochondrion of African trypanosomes. *J. Biol. Chem.* **283**, 27785–27798.
27. Noguera, V., Walker, O., Rouhier, N., Jacquot, J. P., Krimm, I. & Lancelin, J. M. (2005). NMR reveals a novel glutaredoxin–glutaredoxin interaction interface. *J. Mol. Biol.* **353**, 629–641.
28. Kelley, J. J., III, Caputo, T. M., Eaton, S. F., Laue, T. M. & Bushweller, J. H. (1997). Comparison of backbone dynamics of reduced and oxidized *Escherichia coli* glutaredoxin-1 using ^{15}N NMR relaxation measurements. *Biochemistry*, **36**, 5029–5044.
29. Johnson, D. C., Dean, D. R., Smith, A. D. & Johnson, M. K. (2005). Structure, function, and formation of biological iron-sulfur clusters. *Annu. Rev. Biochem.* **74**, 247–281.
30. Lillig, C. H., Berndt, C., Vergnolle, O., Lonn, M. E., Hudemann, C., Bill, E. & Holmgren, A. (2005). Characterization of human glutaredoxin 2 as iron–sulfur protein: a possible role as redox sensor. *Proc. Natl Acad. Sci. USA*, **102**, 8168–8173.
31. Picciocchi, A., Saguez, C., Boussac, A., Cassier-Chauvat, C. & Chauvat, F. (2007). CGFS-type monothiol glutaredoxins from the cyanobacterium *Synechocystis* PCC6803 and other evolutionary distant model organisms possess a glutathione-ligated [2Fe-2S] cluster. *Biochemistry*, **46**, 15018–15026.
32. Rouhier, N., Unno, H., Bandyopadhyay, S., Masip, L., Kim, S. K., Hirasawa, M. *et al.* (2007). Functional, structural, and spectroscopic characterization of a glutathione-ligated [He–2S] cluster in poplar glutaredoxin C1. *Proc. Natl Acad. Sci. USA*, **104**, 7379–7384.
33. Iwema, T., Picciocchi, A., Traore, D. A., Ferrer, J. L., Chauvat, F. & Jacquamet, L. (2009). Structural basis for delivery of the intact [Fe2S2] cluster by monothiol glutaredoxin. *Biochemistry*, **48**, 6041–6043.
34. Johansson, C., Kavanagh, K. L., Gileadi, O. & Oppermann, U. (2007). Reversible sequestration of active site cysteines in a 2Fe-2S-bridged dimer provides a mechanism for glutaredoxin 2 regulation in human mitochondria. *J. Biol. Chem.* **282**, 3077–3082.

35. Johansson, C., Lillig, C. H. & Holmgren, A. (2004). Human mitochondrial glutaredoxin reduces S-glutathionylated proteins with high affinity accepting electrons from either glutathione or thioredoxin reductase. *J. Biol. Chem.* **279**, 7537–7543.
36. Corpet, F. (1988). Multiple sequence alignment with hierarchical clustering. *Nucleic Acids Res.* **16**, 10881–10890.
37. Gouet, P., Robert, X. & Courcelle, E. (2003). ESPript/ENDscript: extracting and rendering sequence and 3D information from atomic structures of proteins. *Nucleic Acids Res.* **31**, 3320–3323.
38. Otwinowski, Z. & Minor, W. (1997). Processing of X-ray diffraction data collected in oscillation mode. *Methods Enzymol.* **276**, 307–326.
39. Brodersen, D. E., Fortelle, E. d. L., Vonrhein, C., Bricogne, G., Nyborg, J. & Kjeldgaard, M. (2000). Applications of single-wavelength anomalous dispersion at high and atomic resolution. *Acta Crystallogr., Sect. D: Biol. Crystallogr.* **56**, 431–441.
40. Adams, P. D., Grosse-Kunstleve, R. W., Hung, L. W., Ioerger, T. R., McCoy, A. J., Moriarty, N. W. *et al.* (2002). PHENIX: building new software for automated crystallographic structure determination. *Acta Crystallogr., Sect. D: Biol. Crystallogr.* **58**, 1948–1954.
41. Emsley, P. & Cowtan, K. (2004). Coot: model-building tools for molecular graphics. *Acta Crystallogr., Sect. D: Biol. Crystallogr.* **60**, 2126–2132.
42. Murshudov, G. N., Vagin, A. A. & Dodson, E. J. (1997). Refinement of macromolecular structures by the maximum-likelihood method. *Acta Crystallogr., Sect. D: Biol. Crystallogr.* **53**, 240–255.
43. Davis, I. W., Leaver-Fay, A., Chen, V. B., Block, J. N., Kapral, G. J., Wang, X. *et al.* (2007). MolProbity: all-atom contacts and structure validation for proteins and nucleic acids. *Nucleic Acids Res.* **35**, W375–W383.
44. Laskowski, R. A., Macarthur, M. W., Moss, D. S. & Thornton, J. M. (1993). Procheck—a program to check the stereochemical quality of protein structures. *J. Appl. Crystallogr.* **26**, 283–291.
45. Ricci, G., Caccuri, A. M., Lo Bello, M., Pastore, A., Piemonte, F. & Federici, G. (1994). Colorimetric and fluorometric assays of glutathione transferase based on 7-chloro-4-nitrobenzo-2-oxa-1,3-diazole. *Anal. Biochem.* **218**, 463–465.